Sol−Gel-Based, Planar Waveguide Sensor for Water Vapor

Peter J. Skrdla,[†] S. Scott Saavedra,*,[†] Neal R. Armstrong,*,[†,‡] Sergio B. Mendes,[‡] and N. Peyghambarian[‡]

Department of Chemistry and Optical Sciences Center, University of Arizona, Tucson, Arizona 85721-0041

A water vapor sensor based on a combination of sol−gel processing and planar optical waveguide technologies has been developed. The indicator erythrosin B was entrapped in a thin sol−gel film (thickness ∼100 nm) prepared from methyltriethoxysilane, dimethyldiethoxysilane, and tetraethoxysilane. This dye exhibits an increase in absorbance in the presence of liquid or gaseous water. The sol−gel layer containing the dye was deposited onto a sol−gel-derived, single-mode planar waveguide. Outcoupled light intensity measurements (at 514.5 nm) over a range of water vapor concentrations (in a nitrogen gas stream) yielded a response over a wide range of relative humidity (<1−∼70%) at room temperature. Response and reversal times were less than 1 min, which may make this sensor attractive for real-time monitoring applications.

The rapid and reversible detection of water vapor in otherwise inert process gas streams (e.g., Ar or N$_2$) and low-pressure environments is an economically significant problem, particularly in industrial processes such as semiconductor manufacturing where water represents an unwanted source of oxygen.[1,2] Currently, mass spectrometry techniques are used widely for trace water vapor detection in process gas streams.[1] Although these techniques have the desired ppb sensitivity under the appropriate conditions, they are costly to implement at multiple sites over several process streams. Low-cost sensors that respond rapidly and reversibly to changes in trace water vapor concentration in process gas streams are clearly needed.

Conductometric and capacitive sensors for water have been reported by several research groups.[3−8] For example, a class of conductometric humidity detectors based on higher valence manganese oxide thin films have been developed.[6] These devices showed good reversibility at 80% RH, with response times of ∼2 min. Saab et al.[8] recently reported that a film derived from oxidation of K$_3$C$_{60}$ produced a conductometric response to water vapor over a range of 0.1−100% RH, with a response time of less than 2 min. (Note that 1% RH corresponds to ∼195 ppm H$_2$O at STP.)

Surface acoustic wave devices coated with hygroscopic polymer films of polyimide and polystyrene sulfonate have also been employed for moisture sensing.[9−11] Nomura et al.[11] observed a linear response for their device between 45 and 90% RH, with a velocity change of 1 m/s for a 1% change in relative humidity. Optical humidity sensors have also been reported.[12−15] Ballantine and Wohltjen[13] constructed a sensor using a glass capillary waveguide coated with a polymer film containing CoCl$_2$. This device responded to relative humidity levels between 60 and 100%, with response times ranging from 47 to 170 s. Morisawa et al.[14] used a phenol red-doped, multilayer Langmuir−Blodgett film as the transducer in an absorbance sensor that responded in less than 1 min to relative humidity values between 15 and 60%. Surface plasmon resonance[15] and planar waveguide devices[12] for sensing refractive index changes caused by water adsorption on the respective transducer surface have been described.

Organically doped sol−gel glasses are useful indicator materials for optical sensing of gaseous analytes, as demonstrated by a number of recent papers.[16−20] Sol−gel-derived materials[20−22] have

* Corresponding author: (voice) (520) 621-9761; (fax) (520) 621-8407; (e-mail) saavedra@u.arizona.edu.

† Department of Chemistry.

‡ Optical Sciences Center.

(1) Tilford, C. R. In *Semiconductor Characterization*; Bullis, W. M., Seiler, D. G., Diebold, A. C., Eds.; AIP Press: Woodbury, NY, 1996; pp 252−255.

(2) Ma, C.; Haider, A. M.; Shadman, F. *IEEE Trans. Semicond. Manuf.* **1993,** *6,* 361−366.

(3) (a) Matko, V.; Donlagic, D. *IEEE Trans. Instrum. Meas.* **1996,** *45* (2), 561−563. (b) Shibata, H.; Ito, M.; Asakursa, M.; Watanabe, K. *IEEE Trans. Instrum. Meas.* **1996,** *45,* 564−569.

(4) Lukaszewicz, J. P. *Sens. Actuators B* **1992,** *B6,* 61−65.

(5) Ogura, K.; Shiigi, H.; Nakayama, M. *J. Electrochem. Soc.* **1996** *143,* 2925−2930.

(6) Xu, C.; Miyazaki, K.; *J. Electrochem. Soc.* **1992,** *139,* L111−L113.

(7) Oommen, T. V. *Proc. Electron./Electron. Insul. Conf., 20th* **1991,** 236−240.

(8) Saab, A. P.; Laub, M.; Srdanov, V. I.; Stuckt, G. D. *Adv. Mater.* **1998,** *10,* 462−465.

(9) Zellers, E. T.; Han, M. *Anal. Chem.* **1996,** *68,* 2409−2419.

(10) (a) Galipeau, D. W.; Vetelino, J. F.; Lec, R.; Feger, C. J. *Sens. Actuators B* **1991,** *B5,* 59−65. (b) Galipeau, D. W.; Vetelino, J. F.; Feger, C. *J. Plast. Film Sheeting* **1992,** *8,* 258−272.

(11) Nomura, T.; Oobuchi, K.; Yasuda, T.; Furukawa, S. *Jpn. J. Appl. Phys., Part 1* **1992,** *31,* 3070−3072.

(12) (a) Lukosz, W.; Stamm, CH. *Sens. Actuators A* **1991,** *25−27,* 185−188. (b) Hoyer, R.; Mangold, C.; Fattinger, Ch.; Heming, M.; Danielzik, B.; Otto, J.; Lohmeyer, M. *Appl. Phys. Lett.* **1994,** *64,* 2791−2793.

(13) Ballantine, D. S.; Wohltjen, H.; *Anal. Chem.* **1986,** *58,* 2883−2885.

(14) Morisawa, M.; Uematsu, H.; Muto, S. *Jpn. J. Appl. Phys., Part 2* **1992** *31,* L1202−L1205.

(15) Weiss, M. N.; Srivastave, R.; Groger, H. *Electron. Lett.* **1996,** *32,* 842−843.

(16) Yang, L.; Saavedra, S. S.; Armstrong, N. R. *Anal. Chem.* **1996,** *68,* 1834−1841.

(17) (a) Liu, H.-Y.; Switalski, S. C.; Coltrain, B. K.; Merkel, P. B. *Appl. Spectrosc.* **1992,** *46,* 1266−1272. (b) Dulebohn, J. I.; Haefner, S. C.; Berglund, K. A.; Dunbar, K. R. *Chem. Mater.* **1992,** *4,* 506−508.

(18) Dunbar, R. A.; Jordan, J. D.; Bright, F. V. *Anal. Chem.* **1996,** *68,* 604−610.

(19) (a) MacCraith, B. D.; McDonagh, C. M.; O'Keefe, G.; Keyes, E. T.; Vos, J. G.; O'Kelly, B.; McGilp, J. F. *Analyst* **1993,** *118,* 385−388. (b) McDonagh, C.; MacCraith, B. D.; McEvoy, A. K. *Anal. Chem.* **1998,** *70,* 45−50.

(20) Lev, O. *Analusis* **1992,** *20,* 543−553.

several properties that make them attractive for use in optical chemical sensing applications, including the following: (i) They are chemically and thermally stable, highly porous, and optical transparent (into the ultraviolet spectrum). (ii) They can be prepared and cured at room temperature, which makes it feasible to incorporate thermally labile organic dopants via physical entrapment or covalent bonding. (iii) The dopants are sterically accessible to analytes that can diffuse into the pores of the material. (iv) The physical and chemical properties of sol–gel materials can be tailored over a wide range simply by varying precursor composition and/or processing conditions.

To achieve rapid response characteristics in a sol–gel-based sensor, the use of a thin indicator layer is preferable to a monolith.[23,24] However, the smaller optical path length characteristic of a thin-film geometry may compromise sensitivity. The tradeoff between sensitivity and response time can be circumvented by using a planar integrated optical waveguide (IOW) as the sensing platform, as reported in previous studies from this group.[16,24] Since the evanescent field of the guided mode that is used to probe an IOW-supported indicator film has a penetration depth on the order of 100 nm, the indicator film should be similarly thin, which means that a rapid response can be obtained. High sensitivity is a consequence of the relatively large optical path length for attenuated total reflection (ATR) spectrometry characteristic of the IOW geometry.[16,24–26]

A sol–gel-derived IOW sensor for water vapor is described in this report. The indicator material, a porous sol–gel layer doped with erythrosin B, is coated on a single-mode, planar IOW. This dye exhibits an increase in absorbance at 514.5 nm in the presence of water vapor, which is detected as a decrease in the intensity of the light guided in the IOW. The detection limit is estimated to be below 1% RH. The response and reversal times are less than 1 min, which may make this approach attractive for real-time monitoring applications.

EXPERIMENTAL SECTION

Waveguide Fabrication and Characterization. Glass microscope slides (Gold Seal, 3010) were scrubbed lightly with a cotton pad in aqueous nonionic surfactant (2% PCC-54, Pierce) and then sonicated for 15 min in type 1 reagent grade water (Barnstead Nanopure, 18.2 MΩ/cm). After rinsing with water, the substrates were immersed into a heated (80 °C) chromic acid bath for 20 min. Finally, the slides were rinsed copiously with type 1 reagent grade water, dried at 100° C for 30 min, and allowed to cool to room temperature. The waveguiding layer was fabricated using a dip-coating process as described in previous papers.[16,24,25] Briefly, the sol was composed of ethanol (100%, Quantum Chemical Co.),

methyltriethoxysilane (MTES, 99%, Aldrich), titanium(IV) butoxide (99%, Aldrich), and silicon tetrachloride (99%, Aldrich) in a volumetric ratio of 200:150:75:14.5. Waveguides were cured in a tube furnace for 20 min at 500 °C in air, yielding a thickness of ~560 nm and a refractive index of ~1.6. These parameters were determined by measuring the TE_0 and TM_0 incoupling angles, assuming a step profile for the refractive index of the guiding layer and a refractive index of 1.51 for the glass substrate.[27] Waveguide propagation loss was analyzed by imaging the scattered light (CCD, Princeton Instruments) of a prism-coupled, TE-polarized 514.5-nm beam from an Ar^+ laser (Coherent Innova 70), as described previously.[25] Loss coefficients were in the range of 0.1–0.2 dB/cm.

Sensor Indicator Layer. Erythrosin B (spirit soluble, 95+%, Aldrich), dissolved in 50.0 mL of ethanol at a concentration of 0.1 mg/mL, was combined with 15.0 mL of the following volumetric ratio of reagents: 7:5:1:2 of dimethyldiethoxysilane (DMES, 97%, Aldrich), MTES, tetraethoxysilane (TEOS, 99.999%, Aldrich), and concentrated HNO_3. The solution was mechanically mixed for 15 min, followed by sonication for 1 min, and then allowed to age quiescently for 48 h at 4 °C.

The sol–gel indicator layer was coated over a ~2.2-cm-long area in the center of the ~7.5-cm waveguide. The ends were left uncoated so that efficient light coupling could be achieved by clamping the coupling prisms directly to the upper surface of the waveguide. The coating was restricted to the center region by masking the ends of the waveguide with a black strippable paint (Universal Photonics). The indicator sol was then dip coated over the exposed center region at a draw rate of 12 cm/min. After the paint was stripped from the ends, the sensor was cured in air at 75 °C for 12 h. Finally, the sensor was immersed in ethanol for 1 h to leach out loosely bound dye from the indicator layer.

Characterization of Indicator Layers. The interference fringe pattern in the visible transmission spectrum of a glass substrate that was coated with an indicator layer on one side was measured using a Cary 5-G spectrophotometer. The refractive index and thickness of the indicator layer was determined from the fringe pattern as described by Manifacier et al.[28] FT-IR transmission spectra of oxidized Si wafers coated with one indicator layer on each side were collected on a Nicolet 550 at 4 cm^{-1} resolution.[25]

Thicker films (~0.4 mm) of erythrosin B-doped sol–gel were prepared to enable transmission UV–visible spectra to be measured with adequate sensitivity. These films were prepared by mixing 0.3 mL of hydrolyzed tetramethylorthosilicate (TMOS, 99+%, Aldrich) (prepared by combining TMOS, water, and 0.048 M HCl in the volume ratios 71:10:1) with an equivalent volume of 26 μM erythrosin B in ethanol. The mixture was allowed to gel (2 days at room temperature) on the wall of a horizontally placed acrylate cuvette. The response of thick sol–gel films to water vapor, ammonia, and carbon dioxide was measured in a transmission geometry using a Hitachi U2000 UV–visible spectrophotometer.

The wettability of both indicator and waveguide sol–gel layers was examined by measuring the contact angle of a stagnant water drop (~30 μL) deposited by a syringe. Images were taken within 30 s of drop deposition using a charge-coupled device camera (TE/

(21) Brinker, C. J.; Scherer, G. W. *Sol–Gel Science*; Academic: San Diego, 1990.
(22) (a) Avnir, D. *Acc. Chem. Res.* **1995**, *28*, 328–334. (b) Wolfbeis, O. S.; Reisfeld, R.; Ochme, I. *Struct. Bonding* (*Berlin*) **1996**, *85*, 51–98. (c) Dave, B. C.; Dunn, B.; Valentine, J. S.; Zink, J. I. *Anal. Chem.* **1994**, *66*, 1120A–1127A.
(23) Narang, U.; Prasad, P. N.; Bright, F. V.; Ramanathan, K.; Kumar, N. D.; Malhotra, B. D.; Kamalasanan, M. N.; Chandra, S. *Anal. Chem.* **1994**, *66*, 3139–3144.
(24) Yang, L.; Saavedra, S. S. *Anal. Chem.* **1995**, *67*, 1307–1314.
(25) Yang, L.; Saavedra, S. S.; Armstrong, N. R.; Hayes, J. *Anal. Chem.* **1994**, *66*, 1254–1263 and references therein.
(26) (a) Saavedra, S. S.; Reichert, W. M. *Anal. Chem.* **1990**, *62*, 2251–2256. (b) Plowman, T. E.; Saavedra, S. S.; Reichert, W. M. *Biomaterials* **1998**, *19*, 341–355.

(27) Saavedra, S. S.; Reichert, W. M. *Appl. Spectrosc.* **1990**, *44*, 1210–1217.
(28) Manifacier, J. C.; Gasiot, J.; Fillard, J. P. *J. Phys. E: Sci. Instrum.* **1976**, *9*, 1002–1004.

CCD-512TK/1, Princeton Instruments, Inc.) and analyzed using IPLAB software (Spectrum, Inc.). Contact angles of $39 \pm 3°$ were measured for both the waveguiding and indicator layers.

Sensor Response to Water Vapor. The optical arrangement was similar to that used by Yang et al.[16] for gaseous iodine sensing. The linearly polarized 514.5-nm line from an argon ion laser (Ion Laser Technology, model 5500AWC) was mechanically chopped at 923 Hz (Palo Alto Research, model 300) and focused into a gastight flow cell (dimensions, 9 cm × 5 cm × 5 cm) mounted on a rotary stage. A coupling prism (SF6, Karl Lambrecht) was clamped to each end of the waveguide sensor, which was mounted in the flow cell. Rotating the cell with respect to the stationary laser beam allowed it to be prism coupled into the TE_0 waveguide mode. The beam intensity at the incoupling prism was 4−5 mW. After propagating through the section of the waveguide coated with the indicator layer, the light was outcoupled at the second prism and directed through an iris and a lens to a photodiode detector (Liconix, model 40D). The distance between the prisms was ~5 cm (although the interaction length of the beam with indicator film was ~2.2 cm—see above). The photodiode output was directed to a signal preamplifier (Oriel, model 70710) and a lock-in amplifier (Stanford Research Systems, model SR830) referenced to the chopper frequency. The lock-in amplifier signal was sampled at 1−3 points/s using an A/D board (National Instruments ATMIO 16L) installed in a PC running Lab Windows software (National Instruments).

Various concentrations of water vapor in a nitrogen stream were generated by bubbling dry N_2 (passed over Drierite) through a liquid water reservoir using a gas disperser. The reservoir was placed in a thermostated bath (Precision, model 181); control of the temperature over the range of 0.1−22.3 °C generated water vapor concentrations ranging from 3800 to 16 500 ppm. Concentrations of water vapor lower than that in equilibrium with liquid water near 0 °C (~3800 ppm at STP) were obtained by diluting the humidified N_2 stream with a second, dry N_2 stream in a gas-mixing manifold. The flow rate into the flow cell in which the sensor was housed was 120 mL/min. The water vapor concentration exiting the flow cell was also measured with a commercial humidity detector (Electrotech Systems, model 514); the measured relative humidity values were found to agree with the calculated values within 5% over a relative humidity range of 1−80%. The sensor response to water vapor was measured along with response and reversal times. The response time was defined as the period required for the output signal to reach 90% of the total signal change. All measurements were made at room temperature under ambient atmospheric pressure (~702 mmHg).

RESULTS AND DISCUSSION

Physical and Chemical Properties of Sol−Gel Indicator Films. The ratio of precursors used to fabricate the indicator layer was selected on the basis of a previous study[16] which showed that a relatively durable (mechanically hard) yet porous sol−gel film that responds rapidly to analyte can be produced by adjusting the extent of cross-linking in the gel. Here the extent of cross-linking was controlled by the ratio of bifunctional (DMES), trifunctional (MTES), and tetrafunctional (TEOS) precursors.

Prior to any use, indicator films were soaked for 1 h in ethanol (in which erythrosin B is very soluble) to remove loosely bound dye. A previous study[24] showed that this time period was sufficient
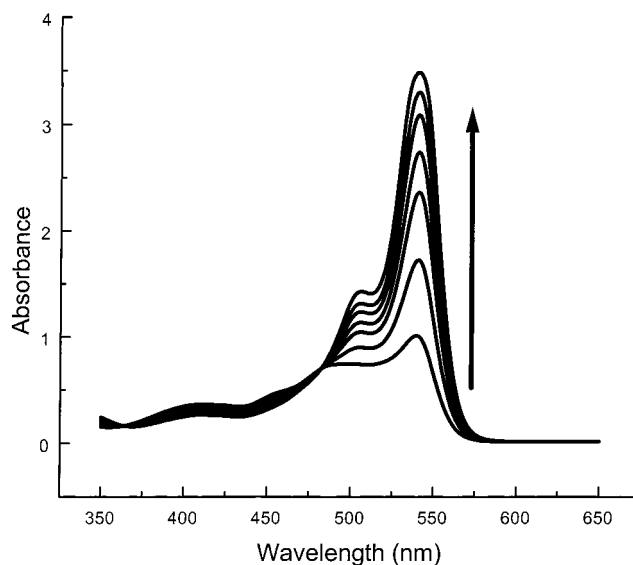
Figure 1. Effect of water on the absorbance spectrum of erythrosin B (0.06 mg/mL) dissolved in ethanol. Spectra were measured for water concentrations of 0, 0.5, 1.0, 1.5, 2.0, 2.4, and 4.8% (v/v). The arrow corresponds to increasing water content.

to extract almost all of the "leachable fraction" of bromocresol purple from a doped sol−gel film prepared using a procedure similar to that used in this work. After the ethanol soak, indicator films were used only in gas-phase environments, so additional indicator leaching did not occur. Absorbance spectrometry of a ~0.4-mm-thick sol−gel layer, doped with erythrosin B and cast on the wall of an acrylate cuvette, showed that, during the ethanol soak, ~20% of the dye was removed. Based on a retention of 80% and a layer thickness of 96 nm (for the waveguide sensing layer—see below), the concentration of erythrosin B in the indicator layer of the sensor was ~74 μM (4.5 × 10^{16} molecules/cm³).

UV−visible absorbance spectra of erythrosin B dissolved in ethanol containing varying amounts of water are shown in Figure 1. In 100% ethanol, the absorbance maximum occurs at 541 nm. Upon addition of water, the absorbance increases and the spectral bands undergo a blue shift. In pure water, the absorbance maximum occurs at 526 nm (spectrum not shown). Similar behavior was observed for a ~0.4-mm-thick sol−gel layer doped with erythrosin B that was cast in an acrylate cuvette. Spectra recorded prior to and following exposure of the layer to water vapor are shown in Figure 2. After the cuvette was uncapped and the water vapor allowed to escape, the spectrum reverted to its preexposure appearance. The difference spectrum (inset to Figure 2) showed that the absorbance increase was centered in the 450−550-nm range, which represents a blue shift of ~20 nm from the spectral shift observed for the dissolved dye (Figure 1). A possible mechanism for the observed spectral changes upon introduction of water is an ionization (proton abstraction) reaction between erythrosin B and water. This mechanism, illustrated in Figure 3, is similar to that postulated for phenol red and Reichardt's dye in the presence of water vapor.[14,29] The interaction of these dyes with water is weak and hence easily reversible, which is attractive for the design of a chemical sensor that responds rapidly and reversibly.

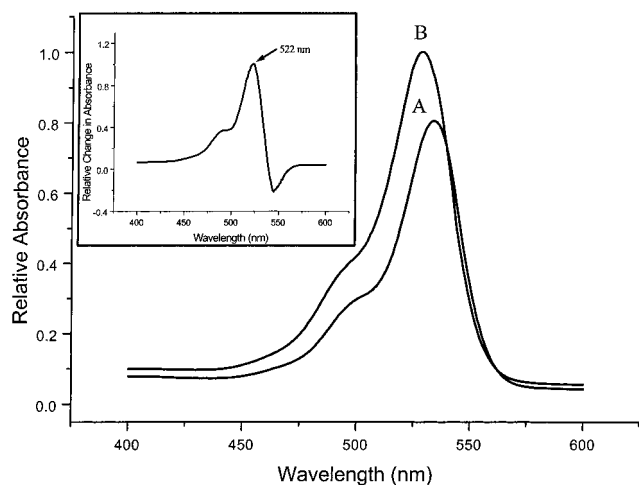(29) Sadaoka, Y.; Sakai, Y.; Murata, Y. *Talanta* **1992**, *39*, 1675−1679.

Figure 2. Absorbance spectra of a ~0.4-mm-thick sol−gel indicator layer doped with erythrosin B that was cast on one wall of an acrylate cuvette. (A) Prior to exposure to water vapor. (B) After placing a few drops of near-boiling water in the bottom of the cuvette. The spectral changes are qualitative, since water vapor was slowly evaporating during acquisition of spectrum B. Plotted in the inset is the difference spectrum (B minus A).
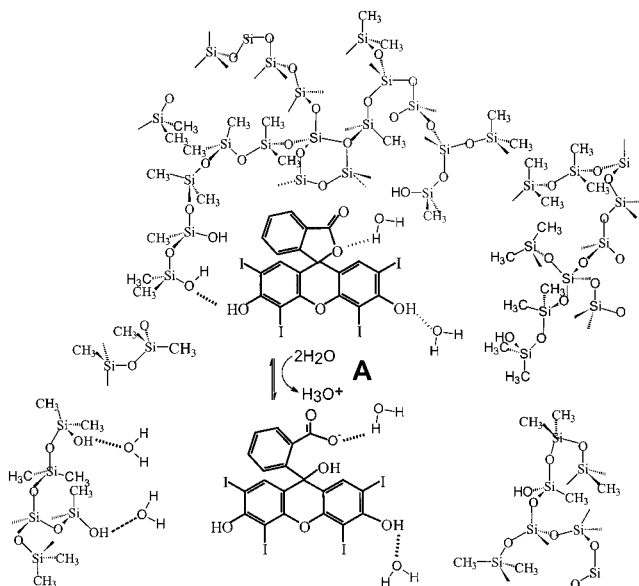

Figure 3. Possible mechanism for interaction of water vapor with an erythrosin B-doped, porous sol−gel is ionization of the dye in the presence of adsorbed water (A), which shifts the visible absorbance band of the dye. Water molecules hydrogen bonded to dye molecules and surface silanols are also present.

The stability of the thick indicator films was assessed by storing them in a laboratory environment, at room temperature, at ambient humidity, and exposed to room light, for a period of 9 months. Following this storage period, UV−visible spectra (not shown) showed that the films retained only ~26% of the absorbance measured within 1 week after preparation. Furthermore, the λ_{max} of the visible absorption band was blue-shifted ~35 nm to 455 nm. The long-term stability of the indicator is thus questionable over long periods of time under these conditions.

The thickness and refractive index of an indicator film coated on a glass substrate were 96 nm and 1.43, respectively, as determined using the interference fringe method described by Manifacier et al.[28] Modeling indicates that this thickness is
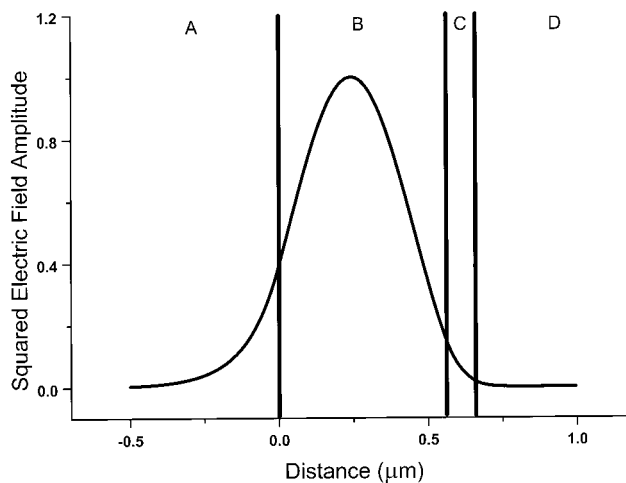

Figure 4. Calculated electric field intensity at 514.5 nm in the TE_0 mode across the laminate structure of the planar waveguide sensor: (A) glass substrate ($n = 1.51$), (B) waveguiding layer ($n = 1.585$, $t = 560$ nm), (C) indicator layer ($n = 1.43$, $k = 6.8 \times 10^{-5}$, $t = 96$ nm), and (D) air superstratum ($n = 1.00$).

appropriate for the planar waveguide sensor described in this study. Plotted in Figure 4 is the electric field intensity in the TE_0 mode across the layers of the waveguide sensor, calculated using a full-wave model.[30] The following parameters were used in the calculation: wavelength 514.5 nm, substrate refractive index 1.51, waveguide thickness 560 nm, waveguide refractive index 1.585, indicator layer thickness and refractive index as given above, attenuation index of the indicator layer (k) = 6.8×10^{-5}, and refractive index of the gaseous superstrate 1.0. The attenuation index was calculated using 9×10^4 M^{-1} cm^{-1} for the molar absorptivity of the dye[31] and 80 μM for dye concentration. Under these conditions, the ratio of the integrated evanescent intensity in the indicator layer to that in the entire superstrata (indicator layer plus gaseous superstratum) was determined to be 0.91. This means that the practical limit for the indicator layer thickness is 100 nm, since the amount of light present in the evanescent field beyond a distance of 100 nm from the waveguiding layer is predicted to be negligible.

Sensor Response to Humidity. The sensor response was assessed using the 514.5-nm output from an Ar laser owing to the ease with which a collimated laser beam can be prism coupled into a planar IOW. The sensor response to alternating exposures of pure nitrogen and 1230 ppm water vapor in nitrogen is shown in Figure 5a. At this concentration, the response was rapid (16 s) and fully reversible (52 s). The response of a sensor to several lower concentrations of water vapor is shown in Figure 5b.

A calibration curve of absorbance measured as a function of ppm water vapor is plotted in Figure 6a. Over the range of 170−~1200 ppm, the response was linear, as shown in Figure 6b. The linear region corresponds to a humidity range of approximately 1−6% RH. At concentrations greater than 1200 ppm, the response became nonlinear, reaching an asymptote at ~5000 ppm (~25% RH). (In this concentration regime, the indicator layer was

(30) (a) Li, L. *J. Opt. Soc. Am. A* **1994**, *11*, 984−991. (b) Li, L. *A User's Guide to BETA*: *A Computer Program for Modeling General Multilayer Planar Waveguides*; University of Arizona, 1994.
(31) Haugland, R. P. *Handbook of Fluorescent Probes and Research Chemicals*, 6th ed.; Molecular Probes, Inc.: Eugene, OR, 1996.
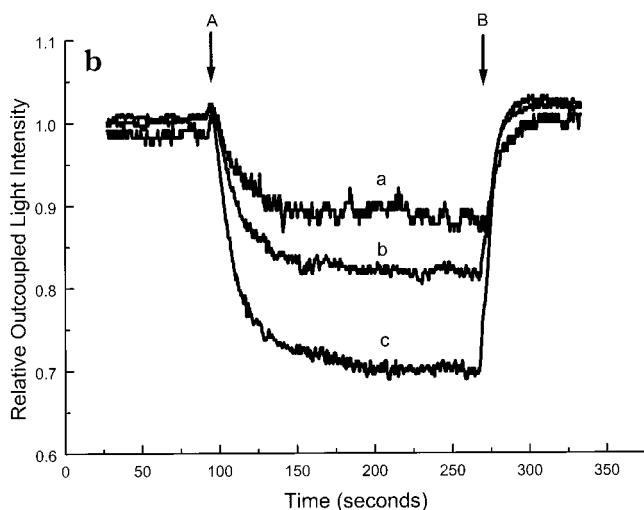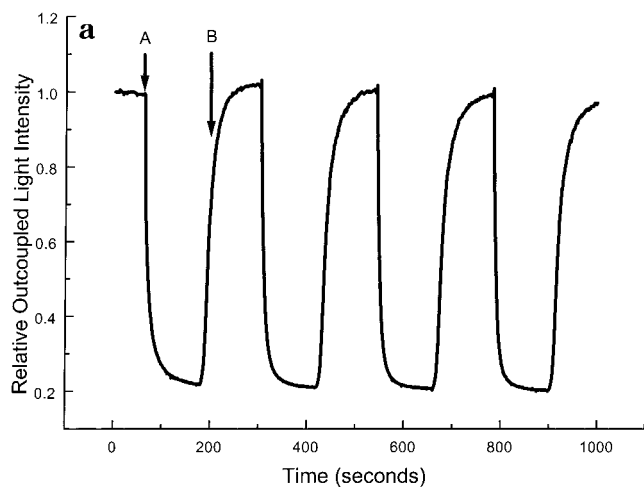
Figure 5. (a) Response at 514.5 nm of the sensor when exposed alternately to (A) 1230 ppm water in a nitrogen gas stream and (B) pure nitrogen. (b) Response at 514.5 nm of the sensor when exposed to (A) water at concentrations of (a) 170, (b) 290, and (c) 420 ppm in a nitrogen gas stream and (B) pure nitrogen.

Figure 6. (a) Calibration curve of absorbance at 514.5 nm measured with the sensor as a function of water concentration in a nitrogen gas stream. The line used in the fit is a logarithmic function; it was employed solely to generate a curve to aid the viewer in visually linking the data points. (b) The linear portion of the calibration curve shown in (a) extends from 170 to 1230 ppm (slope 1.42×10^{-4}, y-intercept -1.34×10^{-2}, correlation coefficient 0.998). The error bars represent standard deviations calculated from the noise in the steady-state sensor response (see examples shown in Fibure 5b).

apparently saturated, given that the measured absorbance of ~0.5 was well below the stray light limit of the optical arrangement.)

When the sensor was exposed to 170 ppm (Figure 5b), the decrease in outcoupled light intensity was 17.5 times greater than the noise in the signal. By extrapolation, the minimum detectable water concentration is predicted to be ~30 ppm. Alternately, from the error in the slope of the calibration curve plotted in Figure 6b, the minimum detectable water concentration is predicted to be ~95 ppm. A more conservative estimate is 115 ppm, which corresponds to a predicted absorbance of 3×10^{-3} au. To our knowledge, these values are far lower than any optical humidity sensor reported to date. However, it is important to note that this sensor has not yet been refined for detection of low water concentrations. Several modifications could be implemented to make the device more sensitive: (i) The optical path length could be increased by coating the indicator layer over a longer region of the waveguide. (ii) The measurement could be performed at a wavelength below 500 nm, where the absorbance change in the presence of water is greater than at 514.5 nm. (iii) The indicator layer could be prepared using a dye that exhibits a greater change in molar absorptivity than erythrosin B when exposed to water
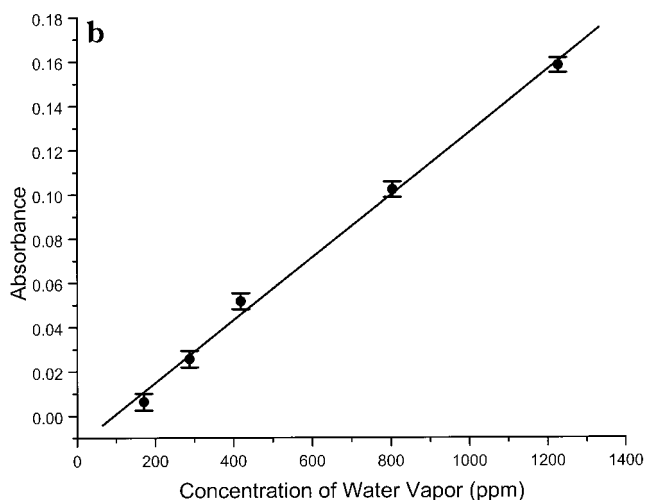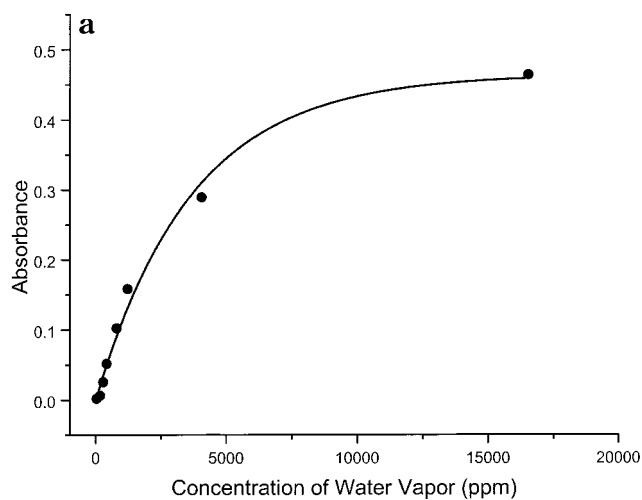
vapor. Some possible candidates are Reichardt's dye[32] and Nile Red.[33] (iv) To compensate for sources of low-frequency drift, both temperature control and intensity referencing could be implemented.

Sensor Response in the Absence of Indicator. An alternate explanation for the sensor response discussed above is that adsorption of water vapor on the walls of the porous indicator layer[34] produces a change in the effective refractive index of the TE_0 waveguide mode. In theory, this change would shift the incoupling angle of the TE_0 mode, which would be detected as an apparent absorbance. Thus the device would not require the presence of a dye in the indicator layer to generate a response to water vapor. Sensors for gaseous analytes based on this principle have been reported by Lukosz and others.[12,35]

(32) Rottman, C.; Grader, G. S.; De Hazan; Y.; Avnir, D. *Langmuir* **1996**, *12*, 5505−5508.

(33) Deye, J. F.; Berger, T. A.; Anderson, A. G. *Anal. Chem.* **1990**, *62*, 615−622.

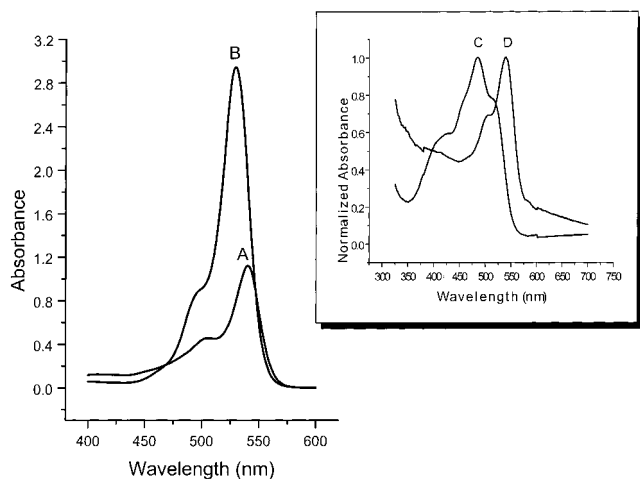(34) Wang, D.; Chong, S. L.; Malik, A. *Anal. Chem.* **1997**, *69*, 9, 4566−4576.

Figure 7. Response of erythrosin B solution (26 μM in 100% ethanol; spectrum A) to the presence of 1% (v/v) ammonium hydroxide (spectrum B). Inset: Response of a ~0.4-mm-thick sol–gel film, doped with erythrosin B (spectrum C), to ammonia vapor (4 min at room temperature) (spectrum D). The absorbance maximums occur at 485 and 538 nm, respectively. Due to clouding of the sol–gel upon exposure to ammonia, spectrum D was background corrected and normalized to spectrum C for clarity of presentation.

To explore this possibility, a planar waveguide sensor was fabricated as described above, except that the indicator layer was not doped with erythrosin B. When this device was exposed to water vapor concentrations of ≤6000 ppm, no measurable decrease in outcoupled light intensity was observed. (The response to concentrations above 6000 ppm was not tested.) The lack of a response in the absence of the indicator dye is not surprising. To measure effective index changes with high sensitivity, a planar IOW must have a high index contrast between the waveguiding and cladding materials and it must be operated near the cutoff condition for single-mode propagation.[12,35] The planar waveguide device described here does not meet these conditions.

Sensor Response to Potential Interferences. The interactions of ammonia and carbon dioxide with dissolved and sol–gel-entrapped erythrosin B were investigated to ascertain potential interferences for the humidity sensor. Introduction of ~1% (v/v) concentrated ammonium hydroxide to a 26 μM solution of erythrosin B dissolved in ethanol resulted in a 2.5-fold increase in absorbance (Figure 7). Note that this response was even greater than the increase observed for 1% water (a ~2.2-fold increase, Figure 1). The inset to Figure 7 shows the response of a ~0.4-mm-thick sol–gel film, doped with erythrosin B, to a 4-min exposure to vapor from concentrated ammonium hydroxide at room temperature. The absorbance maximum red-shifted from 485 to 538 nm, corresponding to an orange-to-pink change in the color of the film. This change of the indicator was accompanied

by clouding of the gel. Both changes were irreversible. Exposure of ~0.4-mm-thick indicator film to CO_2 (prepared by addition of concentrated HCl to an aqueous solution of Na_2CO_3) was also examined. In contrast to the results observed with ammonia, no significant change in the visible spectrum (not shown) of the film was observed. This observation suggests that only Lewis bases stronger than water are likely to be significant interferences for the erythrosin B-based humidity sensor. This argument is consistent with the reaction mechanism shown in Figure 3.

CONCLUSIONS

A planar IOW coated with a dye-doped, porous indicator layer, fabricated using the sol–gel method, can be used to detect water vapor concentrations in the low-ppm range. The combination of sensitivity, response time, and reversibility represents a significant improvement over previous optical humidity sensors. The high sensitivity is characteristic of the single-mode, planar IOW platform. The rapid response and reversibility can be attributed to relatively weak interactions between water molecules and the dye-doped indicator layer, as well as the porosity and submicrometer thickness of the layer. However, strong Lewis bases such as ammonia vapor are potential interferences. Furthermore, the chemical stability of the indicator over a period of several months appears to be problematic. Several modifications (listed above) could be implemented to yield a substantially more sensitive device than the first-generation sensor described here. However, while ppb sensitivity is desirable for applications in the semiconductor processing industry, ppm sensitivity is adequate for numerous other analytical applications.

Finally, we note that although prism coupling was used to launch light into the sensor in this work, this method is not practical for waveguide-based chemical sensing due to inherent reproducibility problems. The use of grating couplers is a better option since they are an integral and permanent part of the waveguide structure and thus provide much better reproducibility and durability. As shown previously by Yang et al.,[16] grating couplers can be readily fabricated in a planar IOW sensing platform of the type described here and should be implemented in any practical application of a planar IOW water vapor sensor. Furthermore, the development of an achromatic grating incoupler for a single-mode, planar IOW by Mendes et al.[36] (*i*) considerably lessens the need to maintain precise alignment between a source and a waveguide grating coupler and (*ii*) makes it feasible to use an inexpensive lamp as the source in a waveguide-based absorbance sensor (rather than the laser used in this study).

(35) (a) Tiefenthaler, K.; Lukosz, W. *Thin Solid Films* **1985**, *126*, 205−211. (b) Tiefenthaler, K.; Lukosz, W. *Opt. Lett.*, **1984**, *10*, 137−139.

(36) (a) Mendes, S. B.; Li, L.; Burke, J. J.; Lee, J. E.; Saavedra, S. S. *Appl. Opt.* **1995**, 34, 6180−6186. (b) Mendes, S.; L. Li, L.; Burke, J.; Lee, J. E.; Saavedra, S. S. *Langmuir* **1996**, *12*, 3374.